

## Effects of three-month feeding high-fat diets with different fatty acid composition on kidney histology and expression of genes related to cellular stress and water-electrolyte homeostasis in mice

A. Wypych<sup>1,\*</sup>, A. Dunisławska<sup>2</sup>, M. Grabowska<sup>3</sup>, K. Michałek<sup>1</sup>, M. Ożgo<sup>1</sup>, K. Liput<sup>4</sup>,  
A. Herosimczyk<sup>1</sup>, E. Poławska<sup>5</sup>, M. Pierzchała<sup>5</sup> and A. Lepczyński<sup>1</sup>

<sup>1</sup> West Pomeranian University of Technology, Faculty of Biotechnology and Animal Husbandry, Department of Physiology, Cytobiology and Proteomics, 71-270 Szczecin, Poland

<sup>2</sup> Bydgoszcz University of Science and Technology, Faculty of Animal Breeding and Biology, Department of Animal Biotechnology and Genetics, 85-084 Bydgoszcz, Poland

<sup>3</sup> Pomeranian Medical University, Faculty of Health Sciences, Department of Histology and Developmental Biology, 71-210 Szczecin, Poland

<sup>4</sup> Institute of Biochemistry and Biophysics, Polish Academy of Sciences, Laboratory of Molecular Basis of Aging and Rejuvenation, 02-106 Warsaw, Poland

<sup>5</sup> Institute of Genetics and Animal Biotechnology, Polish Academy of Sciences, Department of Genomics and Biodiversity, 05-552 Magdalenka, Poland

**KEY WORDS:** alpha-linolenic acid, kidney, linoleic acid, obesity, PUFA, obesity

Received: 27 January 2023

Revised: 22 March 2023

Accepted: 12 April 2023

**ABSTRACT.** The Western diet, which is typically high in saturated fatty acids (SFAs) and low in n-3 polyunsaturated fatty acids (PUFAs), has been identified as a factor contributing to the growing obesity rate. Long-term consumption of high-fat diets (HFDs) has also been associated with increased risk of chronic kidney disease. Therefore, we hypothesized that different fatty acids composition in HFDs would differentially affect renal microstructure and expression pattern of selected genes. Swiss-Webster male mice (n = 24) were fed a standard chow for mice (STD) or HFDs rich in SFAs, and rich in PUFA with a linoleic acid (LA) to  $\alpha$ -linolenic acid (ALA) ratio of 14:1 (HR) or 5:1 (LR) for 3 months. We observed that both the SFA and HR groups had increased epithelial cell vacuolisation, collagenous tissue area and number of TUNEL-positive cells, accompanied by elevated *Kim-1* expression in the kidneys. *Sod1* and *Cat* were up-regulated, while *Cox2* was down-regulated in the kidneys of HR mice when compared to the STD group. Both PUFA-rich HFDs down-regulated the *Ren1* and *Agt* genes. The HR diet also caused an increased deposition of AQP2 in the basolateral membrane (BLM) and intracellular space of collecting duct (CD) cells. In both the HR and SFA groups, an increased expression of the *Aqp3* gene and AQP3 protein in CD cells was observed. In conclusion, the findings suggest that higher levels of ALA in the HFD were associated with a reduction in the severity of renal tissue lesions. Diets rich in SFAs or LA have the potential to modify the renal mechanism of facultative urine concentration by altering the expression and/or distribution of AQP2 and AQP3 in the kidneys.

\* Corresponding author:  
e-mail: [agata.grzesiak@zut.edu.pl](mailto:agata.grzesiak@zut.edu.pl)

## Introduction

Obesity is considered a disease of civilisation, which takes the form of an epidemic and continuous to be a major public health concern. Its development is clearly associated with long-term consumption of high-calorie diets, particularly those rich in saturated fatty acids (SFAs), and limited physical activity (Wickman and Kramer, 2013). Obesity has been proven to be one of the factors contributing to the development of long-term diseases such as chronic kidney disease (CKD), although the complex relationship between obesity and CKD is not yet fully elucidated (Than et al., 2020). The qualitative composition of dietary fatty acids has a significant impact on metabolism and the ability to accumulate lipids in adipose tissue and other body parts (Duran-Montgé et al., 2008). One of the first dietary recommendations aimed at improving health was based on limiting the consumption of saturated fatty acids in favour of polyunsaturated fatty acids. However, this resulted in an unfavourable increase in the consumption of n-6 fatty acids (Hintze et al., 2012), and a marked reduction in the intake of n-3 fatty acids (Simopoulos, 2008). Current dietary recommendations suggest maintaining an appropriate ratio between n-6 and n-3 fatty acids, i.e. 2–5:1, in the diet (Pischon et al., 2003). This is due to the fact that the metabolism of both groups of acids involves the same set of enzymes, which have a higher affinity for the metabolism of n-6 acids. An elevated ratio of n-6 to n-3 acids causes an increase in the synthesis of active metabolites of arachidonic acid, belonging to the n-6 group, showing mainly pro-inflammatory and pro-oxidant effects, while limiting the production of n-3 acid metabolites with anti-inflammatory and antioxidant properties. This imbalance can lead to the development of chronic metabolic diseases (Liput et al., 2021).

It has been proven that the development of chronic kidney disease resulting from high-calorie or high-fat diets is associated with disturbances in cell energy metabolism. Excessive supply of fatty acids impairs mitochondrial function, leading to disruptions in the electron transport chain and generation of reactive oxygen species. As a result, structural changes occur in mitochondrial cristae, reducing the intensity of  $\beta$ -oxidation of fatty acids. Unmetabolised fatty acids are deposited in the cells of renal tubular epithelium in the form of lipid droplets rich in triacylglycerols (Tang et al., 2016). This excess of lipids contributes to oxidative stress, which decreases the activity of enzymes involved in the

detoxification of reactive oxygen species (Costa et al., 2020). Oxidative stress can activate mechanisms associated with the development of inflammation, leading to numerous changes in the kidney microstructure, including increased collagen deposition, epithelial cell vacuolisation, thickening of the glomerular basal membrane, enlargement of mesangial cells of the glomerulus, autophagy and/or apoptosis of glomerular vascular endothelial cells and tubular epithelial cells (Kume et al., 2007; Szeto et al., 2016). It is worth noting that the pro-inflammatory effect of high-fat diets based on saturated fatty acids (SFAs) can be inhibited by supplementation with docosahexaenoic acid (DHA), which belongs to the n-3 fatty acid series (Huang et al., 2012).

We therefore hypothesized that feeding mice with high-fat diets with varying fatty acid compositions for three months would have a distinct impact on the histological structure of their kidneys and the expression of genes involved in cell protection against oxidative stress, inflammation, water-electrolyte homeostasis, and polyunsaturated fatty acids (PUFA) metabolism. The diets were categorized based on their fatty acid composition as follows: (i) high in saturated fatty acids, (ii) high in PUFA with a disturbed n-6/n-3 fatty acid ratio (14:1), and (iii) with a normal ratio of these fatty acids (5:1). Therefore, the objective of this study was to investigate the effect of high-fat diets differing in fatty acid composition on the health status of the kidneys.

## Material and methods

### Animals, diets, housing conditions, experiment termination

The experimental procedures were approved by the 2nd Warsaw Local Ethics Committee for Animal Experimentation (decision no. WAW2\_22/2016). The housing and feeding conditions of the animals were previously described by Lepczyński et al. (2021). Briefly, the experiment included 24 male Swiss-Webster mice, which were housed under controlled temperature and humidity with a 12-h light/dark cycle with free access to water. Before the experiment, animals were fed a standard growth diet for mice from 2 to 10 weeks of age. The animals were then randomly assigned to one of four groups ( $n = 6$ ) and received their specific diets for 3 months. The control group (STD) was fed Labofeed H, a standard mouse feed (Morawski, Żurawia, Poland) with a total fat content of 4.2% in fresh weight. Three other groups were given high-fat diets (HFDs)

containing approx. 24% of total fat content with varying qualitative fatty acid composition obtained by adding suitable plant oils to the standard diet. Once the oils were added, each diet was homogenized and the resulting feed was divided into aliquots, vacuum packed and stored in the dark. The first experimental group was fed a HFD rich in saturated fatty acids (SFA group) based on the addition of virgin coconut oil. The other HFDs were rich in PUFA, but one of them was prepared by adding pumpkin seed oil rich in n-6 fatty acid, resulting in a dietary LA/ALA ratio of 13.76:1 (high ratio, HR group). The last experimental group received a diet with the addition of a plant oil mixture, resulting in a LA/ALA ratio of 5:1 (low ratio, LR group). Table 1 provides information on the macronutrient composition of the control and experimental diets, while Table 2 summarises the main constituents of HFD preparations. Qualitative and quantitative analysis of FA composition in HFDs was performed using a GC-7890 gas chromatograph (Agilent Technologies, Inc., Santa Clara, CA, USA) with a flame ionization detector (FID). The chromatograph utilized a 60 m capillary

column with an internal diameter of 0.25 mm and a stationary phase thickness of 0.20  $\mu\text{m}$  (Hewlett-Packard-88, Agilent J&W GC Columns, Santa Clara, CA, USA). Helium, with the flow rate set at 50 ml/min, was used as a carrier gas. The temperature of the injector and detector was set to 260 °C. The temperature program applied in the analysis was as follows: 1) from 140 °C to 190 °C (4 °C/min), 2) from 190 °C to 215 °C (0.8 °C/min). The FA content was determined against Supelco 37 Component FAME Mix, 47885-U standard (Sigma-Aldrich Co., Saint Louis, MO, USA). The animals were given all diets twice daily to avoid FA oxidation. After a 12-hour overnight fast, the animals were weighed at the end of the feeding trial, and euthanised using a UNO Euthanasia Unit (Uno Roestvaststaal BV, Zevenaar, Netherlands). Carbogen gas (mixture of 95% O<sub>2</sub> + 5% CO<sub>2</sub>) was first introduced into the cage to obtain maximal saturation of blood with oxygen. Then, the carbogen flow was stopped and 100% CO<sub>2</sub> was introduced into the cage to euthanise the animals. After euthanasia, the kidneys were immediately collected and weighed. The left kidney was subjected to histological analysis, and the right kidney was used for mRNA isolation.

**Table 1.** Macronutrient composition of control and experimental diets

Nutrient, %	Control diet	HFDs		
	STD	SFA	HR	LR
Protein	22	17.4	17.4	17.4
Fat	4.2	24.3	24.3	24.3
Fibre	3.5	2.8	2.8	2.8
Ash	5.7	4.5	4.5	4.5

HFDs – high-fat diets; STD – labofeed H, standard chow for mice; SFA – HFD rich in saturated fatty acids; HR – HFD rich in polyunsaturated fatty acids (PUFA) with a linoleic acid (LA) to  $\alpha$ -linolenic acid (ALA) ratio of 14:1; LR – HFD rich in PUFA with a LA to ALA ratio of 5:1

## Histological analyses

The dissected mouse kidneys were routinely fixed in 4% buffered formaldehyde for at least 24 h, washed in a graded ethanol series and xylene. The specimens were embedded in paraffin blocks and cut into 3  $\mu\text{m}$  sections, which were transferred onto poly-lysine slides. Before each staining, the kidney sections were deparaffinised in xylene and rehydrated in decreasing ethanol concentrations.

**Table 2.** Experimental high-fat diets (HFDs) and their fatty acid composition\*

Group	Components	g	LA/ALA	% SFA <sup>1</sup>	% PUFA	% MUFA
SFA <sup>2</sup>	Labofeed H	790	1.41	76.87	11.04	12.09
	virgin coconut oil	200				
	pumpkin seed oil	10				
HR	Labofeed H	790	13.76	1.68	82.21	16.10
	pumpkin seed oil	210				
LR	Labofeed H	790	5.00	9.91	79.69	10.40
	sunflower seed oil	80				
	pumpkin seed oil	65				
	avocado oil	20				
	virgin coconut oil	20				
	hemp seed oil	15				
	maize oil	10				

\* according to the co-author of the present article – Lepczyński et al. (2021); LA/ALA – ratio of linoleic acid (LA, 18:2n-6) to  $\alpha$ -linolenic acid (ALA, 18:3n-3); SFA<sup>1</sup> – saturated fatty acids; MUFA – monounsaturated fatty acids; PUFA – polyunsaturated fatty acids; SFA<sup>2</sup> – animals fed HFD rich in saturated fatty acids; HR – animals fed HFD rich in PUFA with a LA to ALA ratio of 14:1; LR – animals fed HFD rich in PUFA with a LA to ALA ratio of 5:1

The sections were then stained with haematoxylin and eosin (H&E) (Sigma-Aldrich Co., Saint Louis, MO, USA) to visualise the general kidney architecture, and with Masson trichrome (Sigma-Aldrich Co., Saint Louis, MO, USA) to show collagen fibres.

### TUNEL assay

The terminal deoxynucleotidyl transferase dUTP nick-end labelling (TUNEL) assay was performed according to the manufacturer's instructions (ApopTag® Peroxidase In Situ Apoptosis Detection Kit; Millipore, Billerica, MA, USA) to detect nuclear DNA fragmentation related to apoptosis. Kidney sections were deparaffinised, rehydrated and digested with proteinase K. The activity of endogenous peroxidase was blocked by treating all slides with 0.3% hydrogen peroxide in methanol (30 min). The slides were then incubated with terminal deoxynucleotidyl transferase (TdT; Millipore™, Billerica, MA, USA) for 60 min at 37 °C in a humid chamber. After washing with PBS, the slides were incubated with peroxidase-conjugated antidigoxigen antibody for 30 min in a humid chamber. Diaminobenzidine was used to visualise the reaction. Finally, the slides were counterstained with Mayer's haematoxylin, dehydrated and coverslipped. A negative control was also included. The sections were examined under a light microscope (Olympus BX 41, Hamburg, Germany).

### Quantitative analysis of morphological parameters, Masson's trichrome staining and TUNEL-positive cells

Slides stained with H&E and Masson's trichrome, and immunolabelled with TUNEL were scanned at a magnification of 400 × (resolution of 0.25 µm/pixel) using an ScanScope AT2 scanner (Leica Microsystems, Wetzlar, Germany). The obtained digital images were analysed using an Aperio ImageScope viewer (ver. 11.2.0.780; Aperio Technologies, Vista, CA, USA) on a computer screen.

Glomerular diameter (µm) was assessed using a ruler tool on H&E-stained kidney tissue sections. One hundred and forty renal glomeruli were analysed in each group.

Quantitative collagen analysis in mouse kidneys stained with Masson trichrome and TUNEL stain was carried out using the Positive Pixel Count v9 algorithm (ver. 9.1; Aperio Technologies, Vista, CA, USA). Areas of analyses were delineated manually. The percentage of collagen that was positive in Masson's trichrome staining and the total number of positive nuclei in TUNEL assay were

calculated in 50 random fields for each group, with an average area of 1.73 mm<sup>2</sup> (STD group), 1.54 mm<sup>2</sup> (SFA group), 1.42 mm<sup>2</sup> (HR group), and 1.58 mm<sup>2</sup> (LR group).

### Immunohistochemical analysis of aquaporins (AQPs) expression

Kidney sections (2–3 µm thick) were first deparaffinised with xylene and then rehydrated with a series of increasing ethanol dilutions. Subsequently, 0.3% hydrogen peroxide in methanol was used to block endogenous peroxidase activity. To reveal antigens, sections were boiled for 16 min in 1 mM Tris solution (pH 9.0) with 0.5 mM egtazic acid (EGTA) using a microwave oven. Non-specific Ig binding was prevented by incubating the sections in 50 mM NH<sub>4</sub>Cl for 30 min, followed by antigen blocking (1% BSA, 0.05% saponin, and 0.2% gelatine in PBS). Sections were then incubated with anti-AQPs primary antibodies (AQP2 – NB110-74682, AQP4 – NBP1-87679, Novus Biologicals, LLC, Centennial, CO, USA; AQP3 – ab153694, Abcam, Cambridge, United Kingdom) diluted in 0.01 M PBS with 0.1% BSA and Triton X-100 (overnight, 4 °C). The anti-AQP2, -AQP3, and -AQP4 primary antibodies were used at dilutions of 1:2000, 1:2000, and 1:3000, respectively. Subsequently, the slides were incubated with a complex containing a horseradish peroxidase-conjugated secondary antibody (P0448, Agilent Technologies Inc., Santa Clara, CA, USA) at a dilution of 1:200. Diaminobenzidine in chromogen solution (K3468, Agilent Technologies Inc., Santa Clara, CA, USA) was used for signal development. Mayer's haematoxylin (Sigma-Aldrich Co., Saint Louis, MO, USA) was used as a counterstain. In the final step, all slides were dehydrated and coverslipped. The specificity of immunostaining was confirmed by replacing the primary antibody with IgG from rabbit serum. To ensure consistency, all reactions using a particular antibody were carried out under the same time and condition. Immunostained slides were scanned at a magnification of 400 × (resolution of 0.25 µm/pixel) using a ScanScope AT2 scanner (Leica Microsystems, Wetzlar, Germany). The following algorithms were used for quantitative analyses of AQP expression in selected parts of the kidney: the membrane v9 algorithm (ver. 9.1; Aperio Technologies, Vista, CA, USA) for AQP2-4 expression analysis in the apical and basolateral membranes, and the cytoplasmic v2 algorithm (ver. 2.0; Aperio Technologies, Vista, CA, USA) to analyse AQP2 expression in intracellular space. The percentage of renal tubular cells with strong, moderate, and weak positive immunostaining

in the membranes and intracellular vesicles were calculated. The percentage of cells expressing individual AQP for each group separately was counted in a total of 30 random fields, with 20–30 tubules per field.

### RT-qPCR analysis of gene expression RNA isolation

A tissue fragment ( $n = 5$  per group) was added to 1 ml of Trizol (MRC, Cincinnati, OH, USA) and homogenised using a TissueRuptor (Qiagen GmbH, Hilden, Germany) to isolate RNA. Additional purification was performed using a commercial kit (Universal RNA Purification Kit,

Roche Diagnostics, Basel, Switzerland). Each reaction was conducted in two technical replicates. The primer sequences are presented in Table 3. Genes were selected according to their biological functions related to pro-inflammatory response, oxidative stress response, kidney damage, metabolism of polyunsaturated fatty acids and their metabolites and genes regulating renal function. Relative gene expression analysis was conducted separately for each experimental group using the  $\Delta\Delta C_t$  method with glyceraldehyde 3-phosphate dehydrogenase and actin beta serving as reference genes. Geometric means of the cycle threshold ( $C_t$ ) values of the reference genes were used in the analysis.

**Table 3.** Primer sequences

Gene symbol	Gene name	Forward primer sequence (5'→3')	Reverse primer sequence (5'→3')
<i>Gapdh</i>	Glyceraldehyde 3-phosphate dehydrogenase	TGTGTCCGTCGTGGATCTGA	CCTGCTTCACCACCTTCTTGA
<i>Actb</i>	Actin beta	GAGGTATCCTGACCCTGAAGTA	CACACGCAGCTCATTGTAGA
<i>Il-6</i>	Interleukin-6	TGGGACTGATGCTGGTGACA	CTA TTTCCACGATTTCCAGAG
<i>Ccl2</i>	Chemokine (C-C motif) ligand 2	CCCAATGAGTAGGCTGGAGA	AAAATGGATCCACACCTTGC
<i>Sod1</i>	Superoxide dismutase 1	GTGATTGGGATTGCGCAGTA	TGGTTTGAGGGTAGCAGATGAGT
<i>Cat</i>	Catalase	GCGTCCAGTGCGCTGTAGA	TCAGGGTGGACGTCAGTGAA
<i>Prdx6</i>	Peroxiredoxin 6	TTGATGATAAGGGCAGGGAC	CTACCATCACGCTCTCTCCC
<i>Kim-1</i>	Kidney injure molecule 1	TCCACACATGTACCAACATCAA	GTCACAGTGCCATTCCAGTC
<i>Cyp2c29</i>	Cytochrome P450, family 2, subfamily c, polypeptide 29	GCTCTCCTACTCCTGCTGAAGT	ATGTGGCTCCTGTCTTGCATGC
<i>Alox5</i>	Arachidonate 5-lipoxygenase	TGTTCCCATGCCCATCCAG	CACCTCAGACACCAGATGCC
<i>Cox2</i>	Cyclooxygenase 2	AGCGAGGACCTGGGTTCCAC	AAGGCGCAGTTTATGTTGTCTGT
<i>Ephx2</i>	Soluble epoxide hydrolase 2	CTGTGGCCAGTTTGAACACG	ATCACTGGCTCGGAAGAAGC
<i>Ren1</i>	Renin 1	GACTCCTGGCAGATCACGAT	ACCTGGCTACAGTTCACAACATATT
<i>Agt</i>	Angiotensinogen	GGAACGACCTCCTGACTTGG	TCAGATTTGCCCTCCGACC
<i>Aqp3</i>	Aquaporin 3	AACCCTGCTGTGACCTTTG	GCTGCTGTGCCTATGAACTG
<i>Lepr</i>	Leptin receptor	CGGAGAGCCACGCAACTT	CAGCCCCGGGCAGTTT

EURx, Gdansk, Poland). RNA quality and quantity were checked by electrophoresis on a 2% agarose gel, and spectrophotometrically using a NanoDrop 2000 (Scientific Nanodrop Products, Wilmington, DE, USA).

### Gene expression analysis

After RNA isolation, cDNA was synthesised using the Maxima First Strand cDNA Synthesis Kit for RT-qPCR (Thermo Scientific, Vilnius, Lithuania) following the manufacturer's recommendations. The obtained cDNA was used for the real-time PCR reaction, which included Maxima SYBR Green qPCR Master Mix (Thermo Scientific, Vilnius, Lithuania), 1  $\mu$ M each primer, and 140 ng of diluted cDNA. The program was run in a LightCycler II 480

### Statistical analysis

All statistical analyses were carried out using Statistica 13.1 software (StatSoft, Kraków, Poland). Quantitative data (glomerular diameter, percentage of collagenous tissue and TUNEL-positive cells, AQP expression) were first analysed for normality using the Shapiro-Wilk test. Since the obtained values did not follow a normal distribution, the Kruskal-Wallis test was used to determine the significance of the differences between the groups, followed by the Dunn multiple comparison test for post hoc analysis. A  $P$ -value  $< 0.05$  was considered statistically significant. Statistical analyses of mRNA expression levels were performed by comparing the  $\Delta\Delta C_t$  value of each experimental group with that of the control group using a t-test ( $P < 0.05$ ).

## Results

At the end of the experimental period, significant differences in body weight gain and final body weight, were observed as an effect of HFD ingestion, as previously reported by Lepczyński et al. (2021). Additionally, significant alterations in total and relative kidney weight were also observed in mice fed HFDs. Total kidney weight was significantly higher in animals from the SFA and LR groups. In contrast, relative kidney weight was significantly lower in animals fed the HR diet. The results of these morphological parameters are summarised in Table 4.

collagen was significantly lower in the STD group than in the SFA ( $P < 0.001$ ) and HR ( $P = 0.015$ ) groups, but no substantial differences were demonstrated between the STD and LR groups (Table 4).

In all mouse kidneys, TUNEL-positive cells (with nuclear DNA fragmentation) were characterised by a brown-stained nuclei (Figure 1M–P). The percentage of TUNEL-positive cells was significantly higher ( $P < 0.001$ ) in the SFA and HR groups than in the control group. However, there was no statistical difference between the STD and LR groups (Table 4).

**Table 4.** Morphological and histological parameters of murine kidneys after three months of feeding standard (STD) and experimental high-fat diets (HFDs)

Parameter	Diets				
	STD	SFA	HR	LR	
Body weight, g*	35.0 <sup>a</sup>	50.8 <sup>b</sup>	47.5 <sup>b</sup>	43.8 <sup>b</sup>	
Total kidney weight, g	0.644 <sup>a</sup>	0.898 <sup>b</sup>	0.711 <sup>ac</sup>	0.755 <sup>c</sup>	
Relative kidney weight, %	1.86 <sup>a</sup>	1.81 <sup>ab</sup>	1.50 <sup>b</sup>	1.73 <sup>ab</sup>	
Glomerulus diameter, $\mu\text{m}$	mean $\pm$ SD	62.9 $\pm$ 8.0	63.7 $\pm$ 6.9	62.0 $\pm$ 7.4	
	median (range)	62.6 (47.5–88.5)	63.0 (47.0–82.7)	62.2 (42.7–81.0)	60.2 (46.0–82.1)
Collagen type III, %	mean $\pm$ SD	0.32 <sup>a</sup> $\pm$ 0.24	0.90 <sup>b</sup> $\pm$ 0.57	0.61 <sup>b</sup> $\pm$ 0.55	0.42 <sup>a</sup> $\pm$ 0.32
	median (range)	0.22 (0.05–0.94)	0.79 (0.33–3.59)	0.40 (0.10–2.12)	0.36 (0.03–1.30)
TUNEL-positive cells, %	mean $\pm$ SD	8.0 $\pm$ 5.3	15.8 $\pm$ 4.0	14.1 $\pm$ 2.5	9.4 $\pm$ 5.5
	median (range)	7.7 <sup>A</sup> (0.4–17.6)	16.6 <sup>B</sup> (4.0–23.2)	13.9 <sup>B</sup> (9.3–22.7)	10.4 <sup>AB</sup> (1.0–18.2)

SD – standard deviation; SFA – animals fed HFD rich in saturated fatty acids; HR – animals fed HFD rich in polyunsaturated fatty acids (PUFA) with a linoleic acid (LA) to  $\alpha$ -linolenic acid (ALA) ratio of 14:1; LR – animals fed HFD rich in PUFA with a LA to ALA ratio of 5:1; \* previously reported by the co-author of the present work – Lepczyński et al. (2021); values marked with lowercase letters differ significantly at  $P \leq 0.05$ ; values marked with capital letters differ significantly at  $P \leq 0.01$

Histological observations of kidney structure using light microscopy revealed normal renal architecture in the STD and LR groups. However, in the SFA group, marked structural changes were observed that closely resembled tubulointerstitial nephritis. Interstitial oedema and tubulointerstitial infiltration of inflammatory cells were also recorded. Moreover, renal tubular histopathological changes in the form of intensive cytoplasmic vacuolisation of epithelial cells were observed in mice receiving the SFA and HR diets. However, the intensity of this phenomenon appeared to be highest in the SFA group. Vacuoles in the LR group were infrequent, while in the STD group, few or no vacuoles were observed (Figure 1A–H).

The diameter of the glomerulus did not differ between the groups. Similarly, blue-stained fibres were present in collagen fractions of the kidneys in all groups (Figure 1I–L). The percentage of

Immunohistochemical analysis of kidney sections revealed differences in the expression patterns of AQPs 2, 3 and 4. The corresponding representative slides of immunostained kidney samples are shown in Figure 2, and the graphs visualising these protein expression patterns as percentages of cells with strong, moderate and weak expression in specific cell domains are presented in Figure 3. For AQP2 (Figure 2A–D), a significantly higher expression was observed in the basolateral membrane and intracellular space of collecting duct (CD) cells in the kidneys of the HR group. A relatively high expression of this protein was also observed in the SFA group. Similarly, the expression of AQP3 (Figure 2E–H) was significantly higher in the basolateral membranes of CD cells of mice fed the SFA and HR diets. Regarding AQP4 (Figure 2I–L), a considerably weaker expression was observed in the basolateral domain of kidney CD cells in the SFA group.

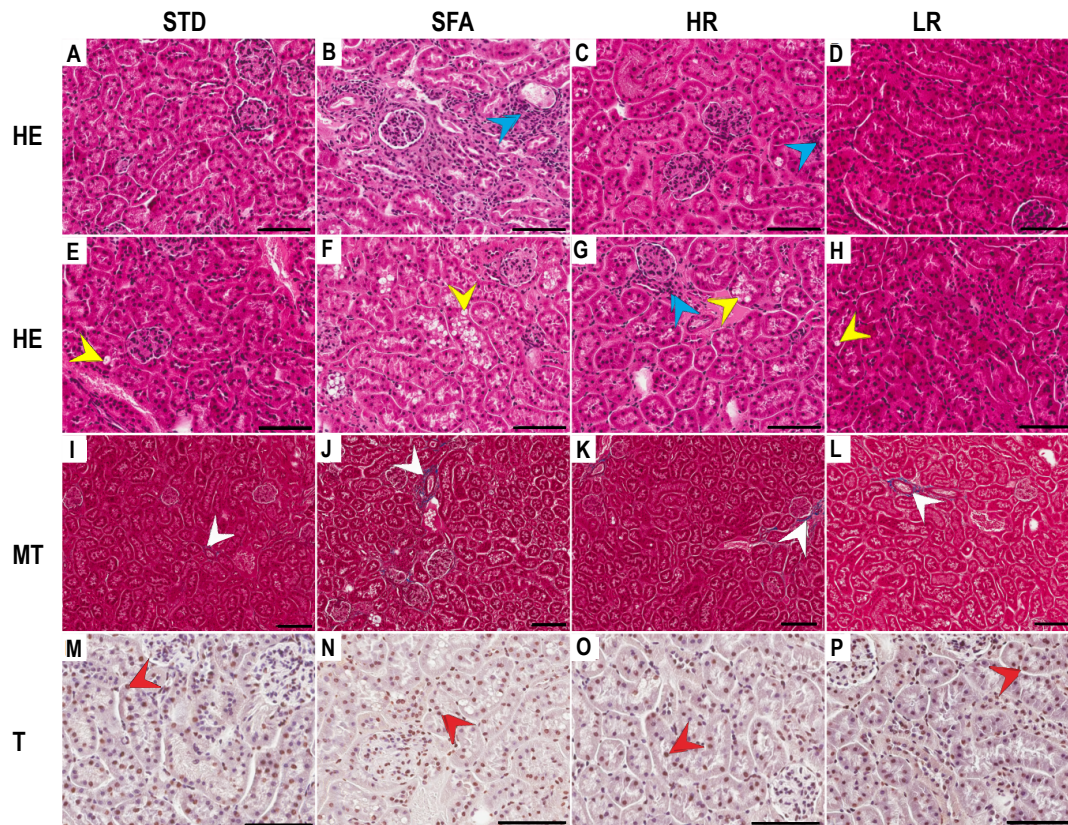


**Figure 1.** Representative light micrographs of kidney cross-sections stained with haematoxylin and eosin (HE; A–H), Masson's trichrome (MT; I–L) and immunostained with TUNEL (T; M–P) after three-months of administration of control (STD; A, E, I, M), SFA (B, F, J, N), HR (C, G, K, O) and LR (D, H, L, P) diets. Normal renal architecture in the STD (A) and LR group (D), interstitial oedema and tubulointerstitial infiltration of inflammatory cells (blue arrowheads) in the SFA (B) and HR (C). Groups few vacuoles (yellow arrowheads) in the STD (E) and LR (H) groups, intense cytoplasmic vacuolisation of renal tubular epithelial cells in the SFA (F) and HR (G) groups. Normal interstitial distribution of collagen fibres (white arrowheads) in the STD (I) and LR (L) groups, increased accumulation of collagen fibres in the SFA (J) and HR (K) groups. TUNEL-positive cells (red arrowheads) in the STD (M), SFA (N), HR (O) and LR (P) groups. Scale bar – 50  $\mu$ m

SFA – animals fed HFD rich in saturated fatty acids; HR – animals fed HFD rich in polyunsaturated fatty acids (PUFA) with a linoleic acid (LA) to  $\alpha$ -linolenic acid (ALA) ratio of 14:1; LR – animals fed HFD rich in PUFA with a LA to ALA ratio of 5:1

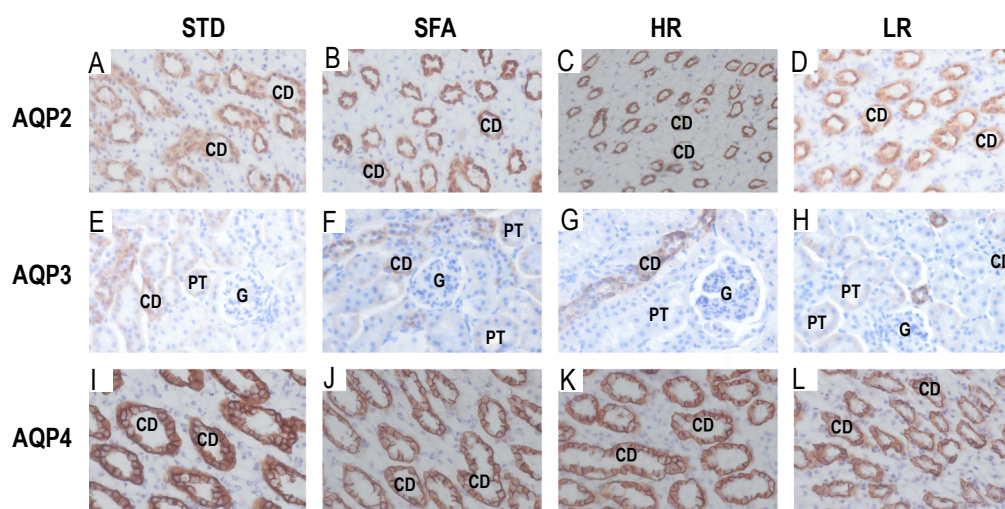


**Figure 2.** Representative light micrographs of immunostained aquaporins (AQPs). Kidney cross-sections after intake of control (STD; A, E, I), SFA (B, F, J), HR (C, G, K) and LR (D, H, L) diets. Different labelling intensities of AQP2 (A–D), AQP3 (E–H) and AQP4 (I–L) were found in collected duct principal cells, and their detailed expression patterns are presented in Figure 3 and described in the text

CD – collecting duct, PT – proximal tubule, G – glomerulus; Scale bar – 50  $\mu$ m; SFA – animals fed HFD rich in saturated fatty acids; HR – animals fed HFD rich in polyunsaturated fatty acids (PUFA) with a linoleic acid (LA) to  $\alpha$ -linolenic acid (ALA) ratio of 14:1; LR – animals fed HFD rich in PUFA with a LA to ALA ratio of 5:1

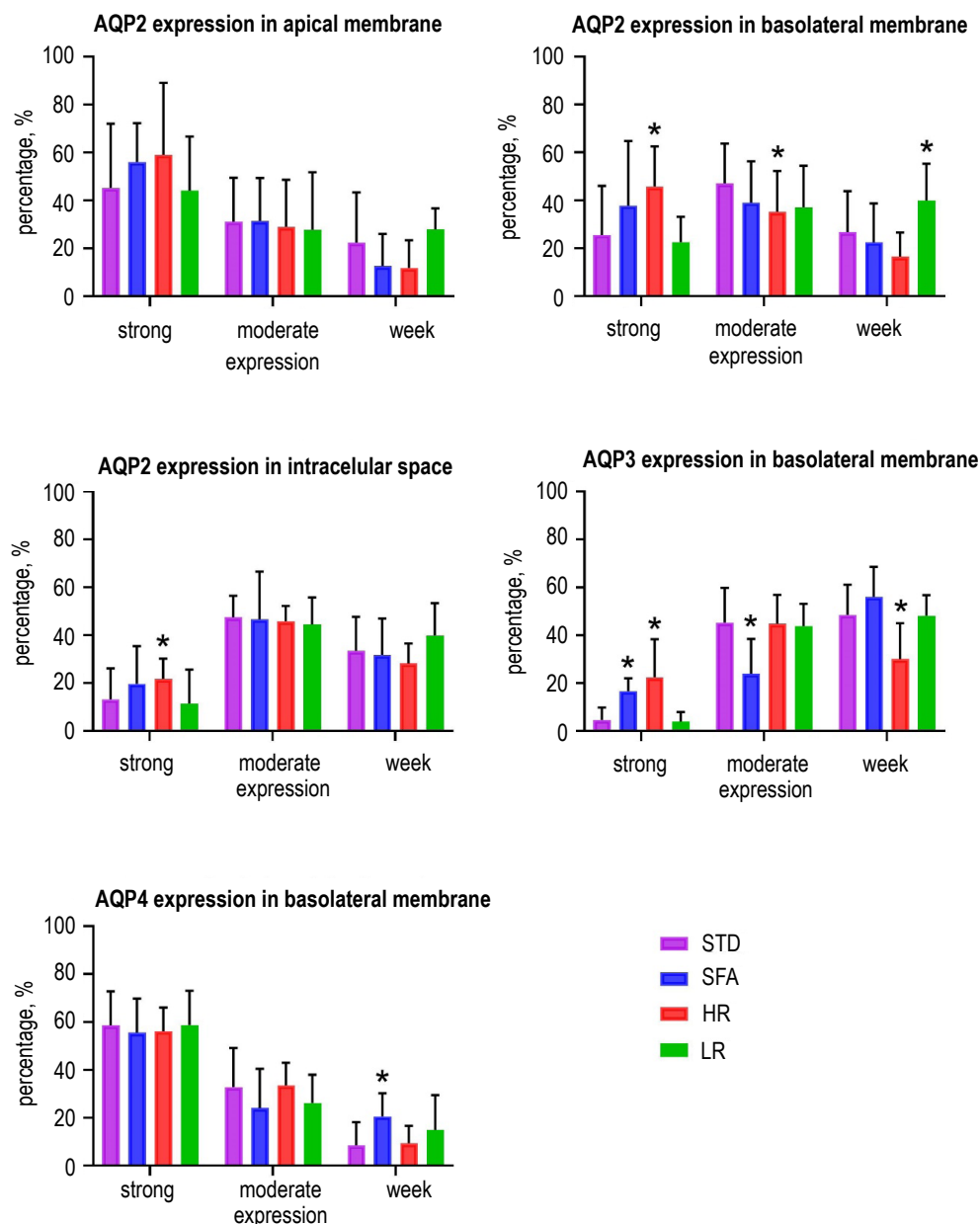


**Figure 3.** Percentage of collecting duct principal epithelial cells with strong, moderate and weak aquaporins (AQPs) 2, 3 and 4 staining signal in mice kidney. AQP2 expression pattern was assessed in the apical membrane, basolateral membrane, and subcellular fraction. AQP3 and AQP4 expression patterns were assessed in the basolateral membrane

STD – labofeed H, standard chow for mice; SFA – animals fed HFD rich in saturated fatty acids; HR – animals fed HFD rich in polyunsaturated fatty acids (PUFA) with a linoleic acid (LA) to  $\alpha$ -linolenic acid (ALA) ratio of 14:1; LR – animals fed HFD rich in PUFA with a LA to ALA ratio of 5:1

The expression patterns of AQPs correspond to the results of AQP immunostainings presented in Figure 2. The results of the expression analysis of the first panel of genes consisting of reporter genes related to kidney damage (*Kim1* – kidney injury molecule 1), oxidative stress (*Sod1* – superoxide dismutase 1, *Cat* – catalase, *Prdx6* – peroxiredoxin 6) and inflammatory genes (*Il6* – interleukin-6, *Ccl2* – chemokine (C-C motif) ligand 2) in the kidneys of mice are presented in Figure 4A, while Figure 4B summarises the results of the analysis

of the second panel of genes involved in energy metabolism (*Lepr* – leptin receptor) and the metabolism of PUFAs and their metabolites (*Cyp2c29* – cytochrome P450, family 2, subfamily c, polypeptide 29, *Alox5* – arachidonate 5-lipoxygenase, *Cox2* – cyclooxygenase 2, *Ephx2* – soluble epoxide hydrolase 2). Finally, Figure 4C presents the analysis of the third panel of genes associated with the regulation of renal function (*Ren1* – renin 1, *Ang* – angiotensinogen, *Aqp3* – aquaporin 3).

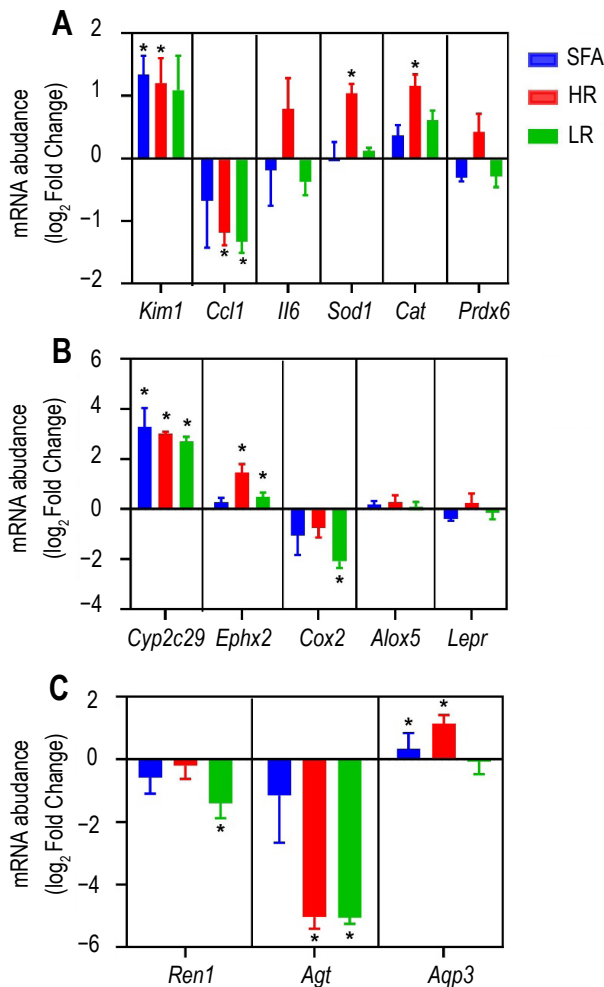


**Figure 4.** Differences in relative gene expression in the kidneys of mice fed high-fat diets (HFDs) with different qualitative fatty acids composition compared to the control group. Panel: A) genes related to cytokines, stress response and kidney injury; B) genes related to lipid and PUFA metabolism; C) genes related to the renin-angiotensin-aldosterone system and water balance. Student's t-test was performed to determine significant differences between experimental and control groups; \* indicates significantly different ( $P < 0.05$ ) values

SFA – animals fed HFD rich in saturated fatty acids; HR – animals fed HFD rich in polyunsaturated fatty acids (PUFA) with a linoleic acid (LA) to  $\alpha$ -linolenic acid (ALA) ratio of 14:1; LR – HFD rich in PUFA with a LA to ALA ratio of 5:1; *Kim1* – kidney injury molecule 1; *Ccl2* – chemokine (C-C motif) ligand 2; *Il-6* – interleukin-6; *Sod1* – superoxide dismutase 1; *Cat* – catalase; *Prdx6* – peroxiredoxin 6; *Cyp2c29* – cytochrome P450, family 2, subfamily c, polypeptide 29; *Ephx2* – soluble epoxide hydrolase 2; *Cox2* – cyclooxygenase 2; *Ephx2* – soluble epoxide hydrolase 2; *Alox5* – arachidonate 5-lipoxygenase; *Lepr* – leptin receptor; *Ren1* – renin 1; *Aqp3* – aquaporin 3

## Discussion

The qualitative composition of the diet has a significant impact on bodily functions. A HFD has been linked to the development of obesity, changes in the weight of internal organs, including the kidneys, and the risk of metabolic disorders, which may eventually lead to kidney damage and

their dysfunction (Deji et al., 2009). Feeding mice a HFD has been found to cause changes in morphometric parameters, such as excess body weight or a decrease in relative kidney mass, regardless of FA source in the HFD (Kasiske et al., 1991). High-fat diets, in addition to changes in morphometric parameters, affected the microanatomical structure of the kidney. Structural changes included renal glomerular fibrosis involving deposition of collagen fibres, enlargement of the glomerular capsule space, expansion of the glomerular mesangium, lipid deposition and abnormal vacuolisation in tubular epithelial cells, inflammation induction, mononuclear cell infiltration, and consequent damage to the renal parenchyma (Deji et al., 2009). The experiment showed that the administration of HFD with a high proportion of SFA and n-6 FA caused significant changes in kidney microarchitecture with local tubulo-interstitial lesions, including tubular epithelial cell (TEC) vacuolisation, increased TEC apoptosis/autophagy rate and higher collagen deposition. However, such changes were not observed in animals fed the LR diet. These observations were reflected in the expression level of the *Kim-1* gene, a known marker of tubular epithelial cell impairments (Zhao et al., 2019). This in turn indicated that the qualitative composition of fatty acids, including the n-6 to n-3 ratio in high-fat diets had a significant effect on the induction of pathophysiological processes in the kidneys. Studies of other researchers analysing the effect of HFD on the kidneys of experimental animals also showed tubular interstitial changes (We et al., 1999), as well as lipid deposition in renal tubular epithelial cells leading to lipotoxicity, increased oxidative stress with induction of programmed cell death of these cells (Sun et al., 2020). Studies have also shown that HFDs with varying qualitative compositions exert different effects on kidney histology. For example, Kasiske et al. (1991) observed that the application of a HFD based on n-3 PUFAs in the form of fish oil did not adversely affect kidney morphology, unlike a diet rich in SFA derived from coconut oil or beef tallow. Metabolites of n-3 PUFAs exerts antioxidative properties (Richard et al., 2008) that attenuate cellular stress and strongly reduce inflammatory signalling. Moreover, n-3 PUFAs and their metabolites may attenuate the development of renal fibrosis by suppressing interstitial fibroblasts activity (Zeng et al., 2017). In addition, n-3 PUFA supplementation was shown to promote fatty acid  $\beta$ -oxidation efficiency (Rombaldova et al., 2017). These properties of n-3 PUFA

and their metabolites could be key factors mitigating the negative effects observed in the SFA and HR groups, namely elevated intracellular vacuolisation, increased collagen deposition and the subsequently enhanced tubular cell apoptosis rate observed in the kidney of mice fed the high-fat diet as opposed to the animals from the LR group.

Feeding HFDs did not significantly affect the expression level of the *Il-6* gene in mouse kidneys. However, a significant reduction in *Ccl2* expression, a gene encoding monocyte chemoattractant protein 1, was observed in the kidneys of mice fed high-fat PUFA diets, while its expression in the kidneys of animals fed the SFA diet remained unchanged. A similar observation was reported by Laurentius et al. (2019), who showed that the use of a HFD based on lard and maize oil in Long-Evans rats for 18 months resulted in structural changes in the kidneys, including infiltrations from immunocompetent cells and monocytes/macrophages, leading to tubular damage and tubulointerstitial fibrosis, with a parallel lack of higher *Ccl2* gene expression in the kidneys and increased protein levels of this gene. The decrease in *Ccl2* gene expression in the kidneys of animals from the HR and LR group could be due to the anti-inflammatory properties of PUFA metabolites (Ulu et al., 2013; Turolo et al., 2021).

An excess of fatty acids in the diet is associated with the induction of oxidative stress, leading to an increase in the activity/expression of the main enzymes responsible for the suppression of oxidative stress, e.g. SOD1 and CAT (Gujjala et al., 2016). This response is likely the effect of the stimulation of mitochondrial biogenesis in the kidneys of animals fed a HFD, as an adaptive mechanism to maintain adequate energy synthesis, which is associated with a considerable increase in the generation of reactive oxygen species (Ruggiero et al., 2011). There are also reports indicating that a significant excess of lipids in the diet may cause not only an increase in the activity/expression of antioxidant enzymes, but also their subsequent suppression after prolonged treatment (Kitada et al., 2020), leading to increased oxidative stress resulting in the development of inflammation and/or induction of renal tubular cell apoptosis (Szeto et al., 2016; Tang et al., 2016). Therefore, it seems that the induction of oxidative stress by LA-rich HFD enhanced the expression of antioxidant enzyme genes, while animals in the SFA group experienced suppression of those genes due to more severe impairment in cellular metabolism; this resulted in vacuolar degeneration in tubular cells and an intensification of programmed death changes in

renal tubular cells. In contrast, this phenomenon was not observed in the LR group, which could be due to a strong antioxidant potential of n-3 PUFAs, unlike the radical-generating n-6 PUFAs and SFAs (Richard et al., 2008).

In the present experiment, a marked increase in the expression of the *Cyp2c29* gene was observed in the kidneys of mice fed each HFD. The results are surprising, as previous studies using HFDs indicated no considerable changes in the expression of CYP2C enzymes in the kidneys (Dey et al., 2004; Luo et al., 2019). However, *Cyp2c29* protein belongs to the cytochrome P450 family and catalyses the synthesis of important active derivatives of n-6 and n-3 acids, EETs (epoxyeicosatrienoic acids) and EDPs (epoxydocosapentaenoic acids), respectively (Calder, 2020). Both EETs and EDPs show significant anti-inflammatory effects, manifested by a reduction in the synthesis of pro-inflammatory cytokines and macrophage flux in the kidneys (Ulu et al., 2013; Turolo et al., 2021). These compounds also influence the activity of the systemic renin-angiotensin-aldosterone system (RAAS) and local renal renin-angiotensin system (RAS) (Ulu et al., 2014). Moreover, *Ephx2* expression in animals fed PUFA-rich HFDs was significantly higher in our study compared to animals fed a standard diet. Soluble epoxide hydrolase (sEH) encoded by *Ephx2* catalyses the conversion of the aforementioned EETs and EDPs to their metabolites with low biological activity (Dufflot et al., 2021). Previous studies have shown that sEH inhibition reduces the degradation of EETs and EDPs, preserving their biological functions, and thus limiting the development of inflammation and HFD-induced kidney damage (Luo et al., 2019). It should be noted that the conversion of most EDPs by sEH to their metabolites is more dynamic compared to EETs, but one of n-3 acid metabolites, 19.20-EDP, shows a high stability and biological activity (Morisseau et al., 2010). This metabolite has been shown to exert antifibrotic effects in the kidneys (Sharma et al., 2016), and may have been responsible for attenuating the negative renal effects of HFD in the LR group.

The current experiment also showed a significant reduction in renal *Cox2* gene expression in the LR group. Previous studies in a rat model have demonstrated that the administration of n-3 acids in animals' diets downregulated COX-2 expression after its prior induction by stress associated with partial nephrectomy. It is important to highlight that the expression of COX-2 is closely linked to the activity of the RAAS, specifically with the level of renin synthesis (An et al., 2009), as it

has been shown that the knockout of the *COX-2* gene led to a decrease in renin expression (Cheng et al., 2001). Therefore, lower *Cox-2* expression in the group of animals fed a high-fat diet with the highest ALA content probably caused a decrease in *Ren1* gene expression in the current study. This concept seemed to be supported by the study, in which the application of three HFDs with different qualitative fatty acid composition had a different effect on renin synthesis in the kidneys; it was reduced by 75% as a result of the addition of n-3-rich linseed oil to the diet, and by 65% when n-6-rich sunflower oil was supplemented compared to animals fed a diet with saturated fatty acids derived from coconut oil (Codde et al., 1984).

Administration of high-fat diets rich in PUFAs reduced the expression of the angiotensinogen gene, another RAAS component. This phenomenon may be explained by the possible activation of peroxisome proliferator-activated receptor  $\gamma$  (PPAR $\gamma$ ) by PUFAs or their metabolites. PUFAs have been shown to be important ligands for receptors with transcription factor activity for PPAR $\gamma$  (Bordoni et al., 2006). On the other hand, an increase in PPAR $\gamma$  activity has been found to downregulate the expression of angiotensinogen and converting enzyme (Roszer and Ricote, 2010).

This study also analysed the expression profile of aquaporins 2, 3 and 4. Aquaporins 2 and 3 are involved in an optional, vasopressin-dependent mechanism of water reabsorption in renal collecting ducts (Mobasheri et al., 2005). In the present study, an increase in AQP2 expression was observed in the basolateral membrane and cytosolic domain of CD cells in the HR group. A similar trend in the expression of this protein was recorded in the SFA group, however, the observed differences were not confirmed statistically due to high deviations from the mean value. For AQP3, its expression was found to be higher at the gene and protein level in the SFA and HR groups. In addition, AQP4 expression was significantly reduced in the HR group. There is limited data on changes in renal aquaporin expression under the influence of high-calorie diets. The observations of Quadri et al. (2016) were consistent with the results obtained in the current study. These authors showed that feeding a high-fat diet increased the expression of AQP2 in renal CD cells. We also believe that chronically elevated plasma vasopressin levels, which accompany obesity (Deligözoğlu et al., 2020), may be another factor contributing to the increased AQP2 expression in the kidneys of the tested mice, along with the translocation of

this protein to the basolateral domain. Studies on the vasopressin analogue 1-deamino-8-D-arginine-vasopressin demonstrated that its chronic 6-day application in rats increased the expression and translocation of this protein to the basolateral membrane of renal collecting tubules (Christensen et al., 2003). The high AQP2 expression in the kidneys of the HR animals may have also resulted from arachidonic acid accumulation in cell membranes. Studies have shown that arachidonic acid may affect the expression of AQP2, also in a vasopressin-independent manner (Ando et al., 2016).

Ewida and Al-Sharaky (2016) found an increase in AQP3 expression in both proximal and distal duct kidney cells in rats under the influence of a high-calorie diet, which they attributed to oxidative stress level and AQP3 permeability to hydrogen peroxide. It appears that the same mechanism related to the regulation of intracellular  $H_2O_2$  concentration may be responsible for the high expression of AQP3 in the current study. AQP3 is a peroxiporins involved in the detoxification of the cells from excess  $H_2O_2$  (Gašparović et al., 2021), indicating the possibility of ROS detoxification in renal tubular cells resulting from lipid metabolism disorders. AQP4 expression determined in the present work was consistent with findings of Halperin Khuns and Pluznick (2018), who observed significant down-regulation of the *Aqp4* gene in the kidney of mice fed a HFD, possibly due to increased cellular ROS synthesis, similarly to AQP3 expression.

## Conclusions

In summary, the study found that high-fat diets with different qualitative fatty acid composition exerted a varying effect on the histological microstructure of the kidneys. A diet based on saturated fatty acids caused the strongest vacuolisation of renal proximal tubular epithelium, with the highest number of cells with the apoptotic features in this segment of the nephron. The severity of these changes was alleviated by increasing levels of alpha linolenic acid in the high-fat diet. The rate of renal epithelial cell vacuolisation and the intensity of apoptosis were reflected in the expression of the *Kim-1* gene, which encodes a damage indicator to renal corpuscles and tubules. The observed pathophysiological changes were probably related to the induction of oxidative stress, as indicated by gene expression levels of antioxidant enzymes – SOD1 and CAT. Furthermore, feeding animals HFDs rich in SFA or n-6 PUFA likely altered the renal

mechanism of facultative urine concentration, as indicated by changes in the expression and/or distribution of AQP2 and AQP3 in mouse kidneys. Finally, the diet with the highest proportion of ALA probably affected the regulation of local renal RAS activity.

## Funding source

This work received financial support from two sources. The dietary experiment was conducted with the support of KNOW (Leading National Research Centre) Scientific Consortium “Healthy Animal – Safe Food”, decision of the Ministry of Science and Higher Education No. 05-1/KNOW2/2015”, grant no. KNOW2015/CB/PRO1/44. The analyses performed were supported by The Rector of the West Pomeranian University of Technology in Szczecin for PhD students of The Doctoral School, grant no. 35/2022.

## Conflict of interest

The Authors declare that there is no conflict of interest.

## References

- An W.S., Kim H.J., Cho K.H., Vaziri N.D., 2009. Omega-3 fatty acid supplementation attenuates oxidative stress, inflammation, and tubulointerstitial fibrosis in the remnant kidney. *Am. J. Physiol.-Renal Physiol.* 297, 895–903, <https://doi.org/10.1152/ajprenal.00217.2009>
- Ando F., Sahara E., Morimoto T. et al., 2016. Wnt5a induces renal AQP2 expression by activating calcineurin signalling pathway. *Nat. Commun.* 7, 13636, <https://doi.org/10.1038/ncomms13636>
- Bordoni A., di Nunzio M., Danesi F., Biagi P.L., 2006. Polyunsaturated fatty acids: From diet to binding to ppar $\alpha$  and other nuclear receptors. *Genes Nutr.* 1, 95–106, <https://doi.org/10.1007/bf02829951>
- Calder P.C., 2020. Eicosanoids. *Essays Biochem.* 64, 423–441, <https://doi.org/10.1042/EBC20190083>
- Cheng H.F., Wang J.L., Zhang M.Z., Wang S.W., McKanna J.A., Harris R.C., 2001. Genetic deletion of COX-2 prevents increased renin expression in response to ACE inhibition. *Am. J. Physiol.-Renal Physiol.* 280, 449–456, <https://doi.org/10.1152/ajprenal.2001.280.3.f449>
- Christensen B.M., Wang W., Frøkiær J., Nielsen S., 2003. Axial heterogeneity in basolateral AQP2 localization in rat kidney: effect of vasopressin. *Am. J. Physiol.-Renal Physiol.* 284, 701–717, <https://doi.org/10.1152/ajprenal.00234.2002>
- Codde J.P., Croft K.D., Barden A., Mathews E., Vandongen R., Beilin L.J., 1984. An inhibitory effect of dietary polyunsaturated fatty acids on renin secretion in the isolated perfused rat kidney. *J. Hypertens.* 2, 265–270, <https://doi.org/10.1097/00004872-198406000-00008>
- Costa M.C., Lima T.F.O., Arcaro C.A., Inacio M.D., Batista-Duarte A., Carlos I.Z., Spolidorio L.C., Assis R.P., Brunetti I.L., Baviera A.M., 2020. Trigonelline and curcumin alone, but not in combination, counteract oxidative stress and inflammation and increase glycation product detoxification in the liver and kidney of mice with high-fat diet-induced obesity. *J. Nutr. Biochem.* 76, 108303, <https://doi.org/10.1016/j.jnutbio.2019.108303>
- Deji N., Kume S., Araki S.I. et al., 2009. Structural and functional changes in the kidneys of high-fat diet-induced obese mice. *Am. J. Physiol.-Renal Physiol.* 296, 118–126, <https://doi.org/10.1152/ajprenal.00110.2008>
- Deligözoğlu D., Kasap-Demir B., Alparslan C., Erbak H., Çatlı G., Mutlubaş F., Alayut D., Soyaltın E., Arslansoyu-Çamlar S., Yavaşcan Ö., 2020. Can we use copeptin as a biomarker for masked hypertension or metabolic syndrome in obese children and adolescents? *J. Pediatr. Endocrinol. Metab.* 33, 1551–1561, <https://doi.org/10.1515/jpem-2020-0240>
- Dey A., Williams R.S., Pollock D.M., Stepp D.W., Newman J.W., Hammock B.D., Imig J.D., 2004. Altered kidney CYP2C and cyclooxygenase-2 levels are associated with obesity-related albuminuria. *Obes. Res.* 12, 1278–1289, <https://doi.org/10.1038/oby.2004.162>
- Duflot T., Laurent C., Soudey A. et al., 2021. Preservation of epoxyeicosatrienoic acid bioavailability prevents renal allograft dysfunction and cardiovascular alterations in kidney transplant recipients. *Sci. Rep.* 11, 3739, <https://doi.org/10.1038/s41598-021-83274-1>
- Duran-Montgé P., Realini C.E., Barroeta A.C., Lizardo R., Esteve-García E., 2008. Tissue fatty acid composition of pigs fed different fat sources. *Animal* 2, 1753–1762, <https://doi.org/10.1017/S1751731108003169>
- Ewida S.F., Al-Sharaky D.R., 2016. Implication of renal aquaporin-3 in fructose-induced metabolic syndrome and melatonin protection. *J. Clin. Diag. Res.* 10, CF06–CF11, <https://doi.org/10.7860/JCDR/2016/18362.7656>
- Gašparović A.Č., Milković L., Rodrigues C., Mlinarić M., Soveral G., 2021. Peroxiporins are induced upon oxidative stress insult and are associated with oxidative stress resistance in colon cancer cell lines. *Antioxidants* 10, 1856, <https://doi.org/10.3390/antiox10111856>
- Gujjala S., Putakala M., Nukala S., Bangeppagari M., Ramaswamy R., Desireddy S., 2016. Renoprotective effect of *Caralluma fimbriata* against high-fat diet-induced oxidative stress in Wistar rats. *J. Food Drug Anal.* 24, 586–593, <https://doi.org/10.1016/j.jfda.2016.01.013>
- Halperin Kuhns V., Pluznick J., 2018. Novel differences in renal gene expression in a diet induced obesity model of diabetic nephropathy. *Am. J. Physiol.-Renal Physiol.* 314, F517–F530, <https://doi.org/10.1152/ajprenal.00345.2017>
- Hintze K.J., Benninghoff A.D., Ward R.E., 2012. Formulation of the Total Western Diet (TWD) as a basal diet for rodent cancer studies. *J. Agric. Food Chem.* 60, 6736–6742, <https://doi.org/10.1021/jf204509a>
- Huang S., Rutkowsky J.M., Snodgrass R.G., Ono-Moore K.D., Schneider D.A., Newman J.W., Adams S.H., Hwang D.H., 2012. Saturated fatty acids activate TLR-mediated proinflammatory signaling pathways. *J. Lipid Res.* 53, 2002–2013, <https://doi.org/10.1194/jlr.D029546>
- Kasiske B.L., O'Donnell M.P., Lee H., Kim Y., Keane W.F., 1991. Impact of dietary fatty acid supplementation on renal injury in obese Zucker rats. *Kidney Int.* 39, 1125–1134, <https://doi.org/10.1038/ki.1991.143>

- Kitada M., Xu J., Ogura Y., Monno I., Koya D., 2020. Manganese superoxide dismutase dysfunction and the pathogenesis of kidney disease. *Front. Physiol.* 11, 755, <https://doi.org/10.3389/fphys.2020.00755>
- Kume S., Uzu T., Araki S.I. et al., 2007. Role of altered renal lipid metabolism in the development of renal injury induced by a high-fat diet. *J. Am. Soc. Nephrol.* 18, 2715–2723, <https://doi.org/10.1681/ASN.2007010089>
- Laurentius T., Raffetseder U., Fellner C., Kob R., Nourbakhsh M., Floege J., Bertsch T., Bollheimer L.C., Ostendorf T., 2019. High-fat diet-induced obesity causes an inflammatory microenvironment in the kidneys of aging Long-Evans rats. *J. Inflamm.* 16, 14, <https://doi.org/10.1186/s12950-019-0219-x>
- Lepczyński A., Ożgo M., Michalek K., Dratwa-Chalupnik A., Grabowska M., Herosimczyk A., Liput K.P., Poławska E., Kram A., Pierzchała M., 2021. Effects of three-month feeding high fat diets with different fatty acid composition on myocardial proteome in mice. *Nutrients* 13, 330, <https://doi.org/10.3390/nu13020330>
- Liput K.P., Lepczyński A., Ogluszka M., Nawrocka A., Poławska E., Grzesiak A., Ślaska B., Pareek C.S., Czarnik U., Pierzchała M., 2021. Effects of dietary n-3 and n-6 polyunsaturated fatty acids in inflammation and cancerogenesis. *Int. J. Mol. Sci.* 22, 6965, <https://doi.org/10.3390/ijms22136965>
- Luo Y., Wu M.Y., Deng B.Q. et al., 2019. Inhibition of soluble epoxide hydrolase attenuates a high-fat diet-mediated renal injury by activating PAX2 and AMPK. *Proc. Natl. Acad. Sci. USA.*, 116, 5154–5159, <https://doi.org/10.1073/pnas.1815746116>
- Mobasher A., Wray S., Marples D., 2005. Distribution of AQP2 and AQP3 water channels in human tissue microarrays. *J. Mol. Histol.* 36, 1–14, <https://doi.org/10.1007/s10735-004-2633-4>
- Morisseau C., Inceoglu B., Schmelzer K., Tsai H.J., Jinks S.L., Hegedus C.M., Hammock B.D., 2010. Naturally occurring monoepoxides of eicosapentaenoic acid and docosahexaenoic acid are bioactive antihyperalgesic lipids. *J. Lipid Res.* 51, 3481–3490, <https://doi.org/10.1194/jlr.M006007>
- Pischoon T., Hankinson S.E., Hotamisligil G.S., Rifai N., Willett W.C., Rimm E.B., 2003. Habitual dietary intake of n-3 and n-6 fatty acids in relation to inflammatory markers among US men and women. *Circulation* 108, 155–160, <https://doi.org/10.1161/01.CIR.0000079224.46084.C2>
- Pozzi A., Ibanez M.R., Gatica A.E., Yang S., Wei S., Mei S., Falck J.R., Capdevila J.H., 2007. Peroxisomal proliferator-activated receptor- $\alpha$ -dependent inhibition of endothelial cell proliferation and tumorigenesis. *J. Biol. Chem.* 282, 17685–17695, <https://doi.org/10.1074/jbc.M701429200>
- Quadri S.S., Culver S.A., Siragy H.M., 2016. (Pro)renin Receptor (PRR) mediates high fat diet-induced hypertension via upregulation of epithelial sodium channel. *Hypertension* 68, 188, [https://doi.org/10.1161/hyp.68.suppl\\_1.p188](https://doi.org/10.1161/hyp.68.suppl_1.p188)
- Richard D., Kefi K., Barbe U., Bausero P., Visioli F., 2008. Polyunsaturated fatty acids as antioxidants. *Pharmacol. Res.* 57, 451–455, <https://doi.org/10.1016/j.phrs.2008.05.002>
- Rombaldova M., Janovska P., Kopecky J., Kuda O., 2017. Omega-3 fatty acids promote fatty acid utilization and production of pro-resolving lipid mediators in alternatively activated adipose tissue macrophages. *Biochem. Biophys. Res. Commun.* 490, 1080–1085, <https://doi.org/10.1016/j.bbrc.2017.06.170>
- Roszer T., Ricote M., 2010. PPARs in the renal regulation of systemic blood pressure. *PPAR Res.* 2010, 698730, <https://doi.org/10.1155/2010/698730>
- Ruggiero C., Ehrenshaft M., Cleland E., Stadler K., 2011. High-fat diet induces an initial adaptation of mitochondrial bioenergetics in the kidney despite evident oxidative stress and mitochondrial ROS production. *Am. J. Physiol. Endocrinol. Metab.* 300, E1047–E1058, <https://doi.org/10.1152/ajpendo.00666.2010>
- Sharma A., Khan M.A.H., Levick S.P., Lee K.S.S., Hammock B.D., Imig J.D., 2016. Novel omega-3 fatty acid epoxygenase metabolite reduces kidney fibrosis. *Int. J. Mol. Sci.* 17, 751, <https://doi.org/10.3390/ijms17050751>
- Simopoulos A.P., 2008. The omega-6/omega-3 fatty acid ratio, genetic variation, and cardiovascular disease. *Asia Pacific J. Clin. Nutr.* 17, 131–134
- Sun Y., Ge X., Li X. et al., 2020. High-fat diet promotes renal injury by inducing oxidative stress and mitochondrial dysfunction. *Cell Death Dis.* 11, 914, <https://doi.org/10.1038/s41419-020-03122-4>
- Szeto H.H., Liu S., Soong Y., Alam N., Prusky G.T., Seshan S.V., 2016. Protection of mitochondria prevents high-fat diet-induced glomerulopathy and proximal tubular injury. *Kidney Int.* 90, 997–1011, <https://doi.org/10.1016/j.kint.2016.06.013>
- Tang C., Cai J., Dong Z., 2016. Mitochondrial dysfunction in obesity-related kidney disease: a novel therapeutic target. *Kidney Int.* 90, 930–933, <https://doi.org/10.1016/j.kint.2016.07.045>
- Than W.H., Chan G.C.-K., Ng J. K.-C., Szeto C.C., 2020. The role of obesity on chronic kidney disease development, progression, and cardiovascular complications. *Adv. Biomarker Sci. Technol.* 2, 24–34, <https://doi.org/10.1016/j.abst.2020.09.001>
- Turolo S., Edefonti A., Mazzocchi A., Syren M.L., Morello W., Agostoni C., Montini G., 2021. Role of arachidonic acid and its metabolites in the biological and clinical manifestations of idiopathic nephrotic syndrome. *Int. J. Mol. Sci.* 22, 5452, <https://doi.org/10.3390/ijms22115452>
- Ulu A., Harris T.R., Morisseau C. et al., 2013. Anti-inflammatory effects of  $\omega$ -3 polyunsaturated fatty acids and soluble epoxide hydrolase inhibitors in angiotensin-II-dependent hypertension. *J. Cardiovasc. Pharmacol.* 62, 285–297, <https://doi.org/10.1097/FJC.0b013e318298e460>
- Ulu A., Stephen Lee K.S., Miyabe C., Yang J., Hammock B.G., Dong H., Hammock B.D., 2014. An omega-3 epoxide of docosahexaenoic acid lowers blood pressure in angiotensin-II-dependent hypertension. *J. Cardiovasc. Pharmacol.* 64, 87–99, <https://doi.org/10.1097/FJC.0000000000000094>
- We R., Laboratories C.R., Zucker O., 1999. A high-fat diet aggravates tubulointerstitial but not glomerular lesions in obese Zucker rats. *Kidney Int.* 56, S150–S152
- Wickman C., Kramer H., 2013. Obesity and kidney disease: potential mechanisms. *Semin. Nephrol.* 33, 14–22, <https://doi.org/10.1016/j.semnephrol.2012.12.006>
- Zeng Z., Yang H., Wang Y., Ren J., Dai Y., Dai C., 2017. Omega-3 polyunsaturated fatty acids attenuate fibroblast activation and kidney fibrosis involving MTORC2 signaling suppression. *Sci. Rep.* 7, 46146, <https://doi.org/10.1038/srep46146>
- Zhao X., Chen X., Zhang Y., George J., Cobbs A., Wang G., Li L., Emmett N., 2019. Kidney injury molecule-1 is upregulated in renal lipotoxicity and mediates palmitate-induced tubular cell injury and inflammatory response. *Int. J. Mol. Sci.* 20, 3406, <https://doi.org/10.3390/ijms20143406>